species selection, and active trends within lineages (*24*). Larger vertebrates comparable to our "dead clades," such as Devonian placoderms and extant sharks (*25*), tend to have low fecundity, high parental investment, and increased energy demands balanced by long life spans, multiple breeding seasons, and wide habitat ranges (*K*-selection) (*1*). Extremes of these traits may confer relative extinction resistance in ecologically depleted times while limiting the potential for speciation (*26*–*28*). Smaller vertebrates, such as holocephalans and ray-finned fishes (*29*), tend to have high reproductive rates, short generation times, and large populations (*r*-selection) (*1*). These traits may increase survival through sheer numbers while promoting diversification via higher variation and population fragmentation (*24*, *26*).

The Mississippian recovery interval favored extreme life histories among survivors, selecting for a bimodal size distribution. In the longer term, larger-bodied but less speciose lineages, such as rhizodonts, remained marginal or went extinct (*5*, *16*). Smaller-bodied, rapidly radiating lineages, such as ray-finned fishes, spread to dominate ecosystems (*13*, *16*). Significant downward shifts in Mississippian chondrichthyan and actinopterygian size distributions suggest that this pattern was mirrored within groups (table S21). The Mississippian approximated a scaled-up ecological succession, in which small, short-lived taxa dominate, whereas larger, longer-lived forms are marginal (*30*).

Scattered observations suggest that this pattern is common during long-term recovery intervals. Gigantic, rare postextinction vertebrates were taken as a sign of ecological restoration (*31*). Shrinkage within postextinction invertebrates (*4*, *6*, *8*) was considered restricted or temporary. The oft-noted tendency for major clades to descend from smaller taxa may be linked to such characteristics of postextinction radiations (*3*, *7*). New, diversifying modern ray-finned fishes were smaller than older, diminished ray-finned fish lineages in the Triassic (*32*). Thus, size-related selection has likely shaped vertebrate biodiversity.

Small, opportunistic taxa eventually give way to larger, longer-lived forms in disturbed ecosystems (*29*). Likewise, Cope's rule trends may be favored during stable, saturated times at some distance from recovery conditions (*2*, *5*, *26*, *27*). This describes the intervals containing Devonian vertebrates, late Mesozoic giants, and later Cenozoic mammals (*2*, *5*, *27*). An overall Phanerozoic Cope's rule (*2*) could result from a greater number and length of stable nonrecovery intervals. Vertebrate size trends appear to result from active selection, probably on life histories, with direction based on long-term conditions and survival.

REFERENCES AND NOTES

1. E. R. Pianka, *Am. Nat.* **104**, 592–597 (1970).
2. N. A. Heim, M. L. Knope, E. K. Schaal, S. C. Wang, J. L. Payne, *Science* **347**, 867–870 (2015).
3. S. M. Stanley, *Evolution* **27**, 1–26 (1973).
4. P. J. Harries, P. O. Knorr, *Palaeogeogr. Palaeoclimatol. Palaeoecol.* **284**, 4–10 (2009).
5. M. Friedman, L. C. Sallan, *Palaeontology* **55**, 707–742 (2012).
6. R. Lockwood, . *Paleobiology* **31**, 578–590 (2005).
7. M. S. Y. Lee, A. Cau, D. Naish, G. J. Dyke, *Science* **345**, 562–566 (2014).
8. J. L. Payne, A. B. Jost, S. C. Wang, J. M. Skotheim, *Evolution* **67**, 816–827 (2013).
9. M. V. Lomolino, *J. Biogeogr.* **32**, 1683–1699 (2005).
10. B. Choo, M. Zhu, W. Zhao, L. Jia, Y. Zhu, *Sci. Rep.* **4**, 5242 (2014).
11. T. W. Dahl *et al.*, *Proc. Natl. Acad. Sci. U.S.A.* **107**, 17911–17915 (2010).
12. J. C. Lamsdell, S. J. Braddy, *Biol. Lett.* **6**, 265–269 (2010).
13. L. C. Sallan, M. Friedman, *Proc. Biol. Sci.* **279**, 2025–2032 (2012).
14. L. C. Sallan, T. W. Kammer, W. I. Ausich, L. A. Cook, *Proc. Natl. Acad. Sci. U.S.A.* **108**, 8335–8338 (2011).
15. L. C. Sallan, M. I. Coates, *Proc. Natl. Acad. Sci. U.S.A.* **107**, 10131–10135 (2010).
16. D. L. Royer, R. A. Berner, I. P. Montañez, N. J. Tabor, D. J. Beerling, *GSA Today* **14**, 4–10 (2004).
17. R. A. Berner, *Am. J. Sci.* **309**, 603–606 (2009).
18. B. Worm, M. Sandow, A. Oschlies, H. K. Lotze, R. A. Myers, *Science* **309**, 1365–1369 (2005).
19. D. M. Raup, *Science* **206**, 217–218 (1979).
20. Materials and methods are available as supplementary materials on *Science* Online.
21. S. M. Stanley, *Proc. Natl. Acad. Sci. U.S.A.* **107**, 19185–19189 (2010).
22. D. Jablonski, *Proc. Natl. Acad. Sci. U.S.A.* **99**, 8139–8144 (2002).
23. P. J. Wagner, G. F. Estabrook, *Proc. Natl. Acad. Sci. U.S.A.* **111**, 16419–16424 (2014).
24. S. M. Stanley, *Proc. Natl. Acad. Sci. U.S.A.* **72**, 646–650 (1975).
25. J. A. Long *et al.*, *Nature* **517**, 196–199 (2015).
26. D. Jablonski, *Science* **231**, 129–133 (1986).
27. J. H. Knouft, L. M. Page, *Am. Nat.* **161**, 413–421 (2003).
28. B. Van Valkenburgh, X. Wang, J. Damuth, *Science* **306**, 101–104 (2004).
29. L. A. K. Barnett, R. L. Earley, D. A. Ebert, G. M. Cailliet, *Mar. Biol.* **156**, 301–316 (2009).
30. J. F. Ponge, *Ecol. Evol.* **3**, 1113–1124 (2013).
31. N. B. Fröbisch, J. Fröbisch, P. M. Sander, L. Schmitz, O. Rieppel, *Proc. Natl. Acad. Sci. U.S.A.* **110**, 1393–1397 (2013).
32. C. Romano *et al.*, *Biol. Rev.* 10.1111/brv.12161 (2014).

ACKNOWLEDGMENTS

We thank G. Hunt for assistance with methods; N. Sheldon for advice on climate models; and T. Kailing, D. Rabosky, M. Friedman, J. Clarke, S. Giles, N. Heim, M. Brazeau, and three anonymous reviewers for discussions. We also thank the University of Pennsylvania, Kalamazoo College, the University of Michigan, and the Michigan Society of Fellows for support. All data are available in the supplementary materials.

SUPPLEMENTARY MATERIALS

www.sciencemag.org/content/350/6262/812/suppl/DC1
Materials and Methods
Supplementary Text
Figs. S1 to S91
Tables S1 to S40
References (*33*–*49*)

4 June 2015; accepted 9 October 2015
10.1126/science.aac7373

SMALL RNAS

MicroRNA-encoded behavior in *Drosophila*

Joao Picao-Osorio,[1] Jamie Johnston,[1] Matthias Landgraf,[2] Jimena Berni,[2] Claudio R. Alonso[1]*

The relationship between microRNA (miRNA) regulation and the specification of behavior is only beginning to be explored. We found that mutation of a single miRNA locus (*miR-iab4/iab8*) in *Drosophila* larvae affects the animal's capacity to correct its orientation if turned upside down (self-righting). One of the miRNA targets involved in this behavior is the *Hox* gene *Ultrabithorax*, whose derepression in two metameric neurons leads to self-righting defects. In vivo neural activity analysis reveals that these neurons, the self-righting node (SRN), have different activity patterns in wild type and miRNA mutants, whereas thermogenetic manipulation of SRN activity results in changes in self-righting behavior. Our work thus reveals a miRNA-encoded behavior and suggests that other miRNAs might also be involved in behavioral control in *Drosophila* and other species.

The regulation of RNA expression and function is emerging as a hub for gene expression control across a variety of cellular and physiological contexts, including neural development and specification. Small RNAs such as microRNAs (miRNAs) (*1*) have been shown to affect neural differentiation (*2*, *3*), but their roles in the control of behavior are only beginning to be explored.

Previous work in our laboratory focused on the mechanisms and impact of RNA regulation on the expression and neural function of the *Drosophila Hox* genes (*4*–*7*). These genes encode a family of evolutionarily conserved transcription factors that control specific programs of neural differentiation along the body axis (*8*–*10*), offering an opportunity to investigate how RNA regulation relates to the formation of complex tissues such as the nervous system.

We used the *Hox* gene system to investigate the roles played by a single miRNA locus (*miR-iab4/iab8*) (*4*, *11*–*16*) on the specification of the nervous system during early *Drosophila* development. This miRNA locus controls the embryonic expression of posterior *Hox* genes (*4*, *11*–*16*). Given that we found no detectable differences in the morphological layout of the main components of the

[1]Sussex Neuroscience, School of Life Science, University of Sussex, Brighton BN1 9QG, UK. [2]Department of Zoology, University of Cambridge, Cambridge CB2 3EJ, UK.
***Corresponding author. E-mail: c.alonso@sussex.ac.uk**

nervous system in late *Drosophila* embryos of wild type and *miR-iab4/iab8*–null mutants [herein Δ*miR* (*14*)] (fig. S3, B to F), we analyzed early larval behavior as a stratagem to probe the functional integrity of the late embryonic nervous system.

Most behaviors in early larva were unaffected by the miRNA mutation (fig. S1 and movies S1 and S2), except self-righting (SR) behavior (Fig. 1, A to C, and movies S3 and S4): miRNA mutant larvae were unable to return to their normal orientation at the same speed as their wild-type counterparts.

By means of selective target overexpression followed by SR phenotype analyses, we identified the *Drosophila Hox* gene *Ultrabithorax* (*Ubx*) (*17*, *18*) as a miRNA target implicated in the genetic control of SR behavior (Fig. 1F). Overexpression of Ubx within its expression domain did not affect any larval behavior tested except SR, which is in agreement with the effects observed in miRNA mutants (Fig. 1, D and E). Analysis of *Ubx* 3′ untranslated region (3′UTR) fluorescent reporter constructs expressed in the *Drosophila* central nervous system (CNS) (fig. S2) indicates that the interaction between *miR-iab4/iab8* and *Ubx* is direct, which is in line with prior observations in other cellular contexts (*11*–*13*).

To identify the cellular basis for SR control, we systematically overexpressed Ubx within subpopulations of neurons (fig. S4). Increased levels of Ubx within the pattern of *Cha(7.4kb)-Gal4*, which largely targets cholinergic sensory and interneurons, phenocopied the miRNA SR anomalies (fig. S4). Further overexpression analysis identified two metameric neurons as the minimal node required for the SR behavior [self-righting node (SRN)] (Fig. 2, A and B).

Several lines of evidence confirm the role of miRNA-dependent *Ubx* regulation within the SRN as a determinant of SR. First, both *Ubx* and miRNA transcripts (*miR-iab4*) derived from the *miR-iab4/iab8* locus were detected within the SRN (Fig. 3, A to C). Second, in the context of miRNA mutation, Ubx protein expression is increased within the SRN (Fig. 3, D to F). Third, reduction of Ubx (*Ubx* RNAi) specifically enforced within SRN cells is able to ameliorate or even rescue the SR phenotype observed in miRNA mutants (Fig. 2C).

Two plausible scenarios arise to explain the effects of *miR-iab4/iab8* in regard to SR behavior.

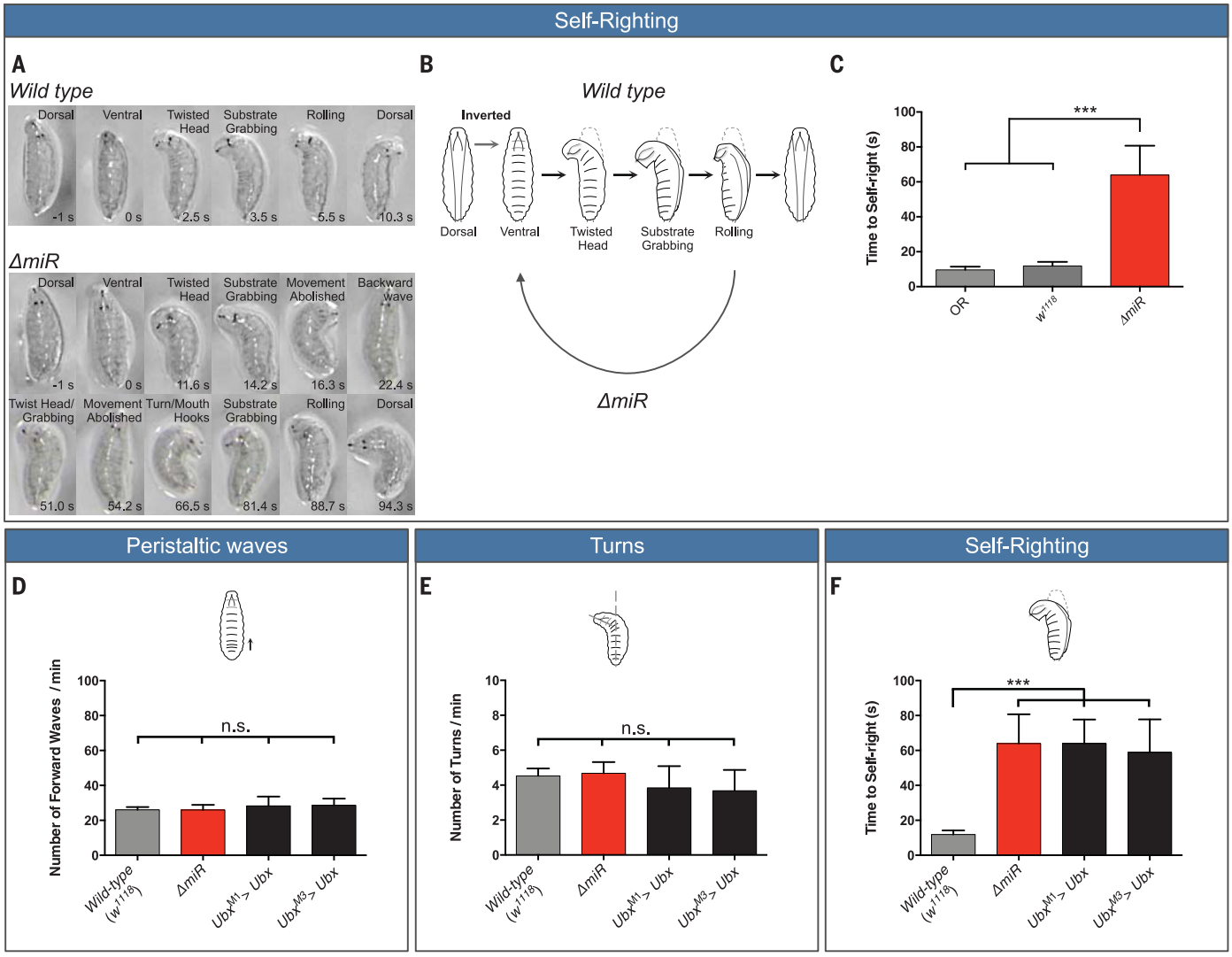

Fig. 1. Both removal of *miR-iab4/iab8* and overexpression of Ubx disrupt a specific larval locomotor behavior: self-righting (SR). (**A** and **B**) Description of larval SR behavior. (A) Time lapses of larval SR behavior. (Top) Wild-type larvae placed in an inverted position (ventral up), twisted their heads, grabbed the substrate with the mouth hooks, and rolled their bodies onto their ventral surface (dorsal up). (Bottom) In contrast, Δ*miR* larvae displayed problems in self-righting their bodies. (B) Diagram of the self-righting behavioral response. (**C**) Quantification of the time required for the successful completion of the SR behavior (mean ± SEM; *n* = 27 to 29 larvae per genotype) in two wild-type controls (*OR* and w^{1118}, light and dark gray, respectively) and Δ*miR* larvae (red). (**D** to **F**) Quantification of larval behavior in Ubx overexpression lines (Ubx^{M1}>*Ubx* and Ubx^{M3}>*Ubx*). Quantification of (D) number of forward peristaltic waves per minute, (E) larval turning per minute, and (F) time to self-right in wild type (w^{1118}, gray), Δ*miR* (red), and Ubx^{M1}>*Ubx* and Ubx^{M3}>*Ubx* (black) (mean ± SEM; *n* = 15 to 29 larvae per genotype). A nonparametric Mann-Whitney *U* test was performed to compare treatments; $P > 0.05$ (nonsignificant; n.s.); $P < 0.001$ (***).

One is that miRNA input is required for the late embryonic development of the neural networks underlying SR, arguing for a "developmental" role of the miRNA; another is that miRNA repression affects normal physiological/behavioral functions largely without disrupting neural development in line with a "behavioral" role. Two independent experiments support that the primary roles of *miR-iab4/8* are behavioral. First, anatomical analysis of SRN cells in wild type (wt), Δ*miR*, and *R54503>Ubx* [SRN-driver line (*19*, *20*)] show no significant differences in total numbers of SRN cells (fig. S5B) or in SRN cell body size (fig. S5C); furthermore, analysis of wt, Δ*miR*, and *R54503>Ubx* show indistinguishable SRN-projection patterns (fig. S5, D and E). Second, Gal-80$_{ts}$–mediated conditional expression experiments show that SRN-specific Ubx overexpression after embryogenesis is sufficient to trigger the SR behavior (Fig. 2, D and E).

The results presented above suggest that miRNA-dependent *Hox* regulation within the SRN must somehow modify the normal physiology of SRN cells so that when the miRNA is mutated, these neurons perform functions different from those in wild-type animals. To test this hypothesis, we used genetically encoded calcium sensors [GCaMP6 (*21*)] specifically expressed in SRN cells and tracked down spontaneous profiles of neural activity. SRN cells in miRNA mutants produce activity traces that are significantly different from those observed in wild-type SRN cells (Fig. 4, B and C, and fig. S6A). Quantification of maximal amplitude and proportion of active cells in each genotype also reveal significant differences (Fig. 4D and fig. S6B) in SRN function across the genotypes, but no change in cell viability is observed (fig. S6C). Neural activity differences across genotypes are significant within regions of expression of *miR-iab4* (Fig. 4E), suggesting that this miRNA (and not *miR-iab8*) might be the main contributor to SR control. Analysis of mutations that selectively affect *miR-iab4* or *miR-iab8* (*14*, *15*, *22*, *23*) strongly suggests that *miR-iab4* is the key regulator of SR (Fig. 3, G and H).

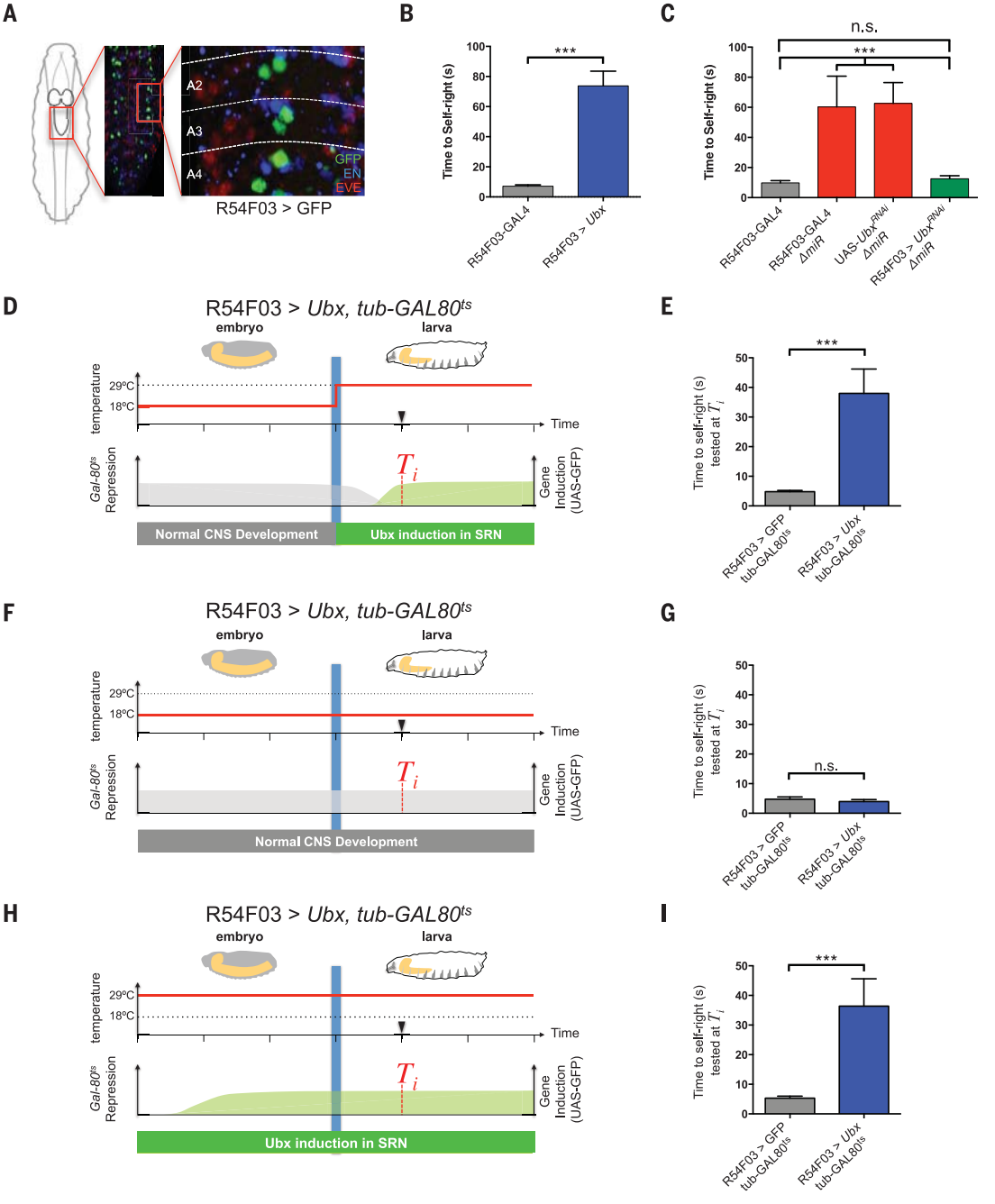

Fig. 2. miRNA-dependent *Ubx* regulation in SRN cells underlies SR behavior. (**A**) *R54F03*-GAL4 expression [green fluoprescent protein (GFP), green] in the larval abdominal CNS. Even-skipped protein is in red; Engrailed protein is in blue; and A2, A3, and A4 refer to abdominal segments 2 to 4, respectively. (**B**) Artificial increase of *Ubx* expression in two metameric neurons driven by the *R54F03* promoter (mean ± SEM; *n* = 60 larvae per genotype). (**C**) Artificial decrease of Ubx expression with Ubx^{RNAi} within SRN cells in Δ*miR* larvae (*R54F03*-GAL4, Δ*miR*/UAS-*Ubx*^{RNAi}, Δ*miR*, green) (mean ± SEM; *n* = 20 to 23 larvae per genotype). (**D** to **I**) Conditional increase of Ubx expression during embryonic and early larval development with *tub*-Gal80^{ts} (Gal80^{ts} represses GAL4 activity at 18°C) within SRN cells: *R54F03* > Ubx, *tub*-GAL80^{ts} (UAS-*Ubx*/+ ; *R54F03*/*tub*-Gal80^{ts}). Controlled increase of Ubx expression in SRN cells in early larvae [(D) and (E); mean ± SEM; *n* = 20 larvae per genotype] and from mid-embryogenesis to early larvae [(H) and (I); mean ± SEM; *n* = 15 larvae per genotype]. [(**F**) and (**G**)] Repressed increase of Ubx expression in SRN cells throughout embryogenesis and early larvae (mean ± SEM; *n* = 15 larvae per genotype). A nonparametric Mann-Whitney *U* test was performed to compare treatments; *P* > 0.05 (nonsignificant, n.s.); ***$P < 0.001$.

To demonstrate that the changes in SRN neural activity were causal to SR behavior, we artificially activated (Fig. 4F) or inhibited (Fig. 4G) SRN cells (*24*, *25*) and showed that this triggered the aberrant SR phenotype. This suggested that activation of SRN cells in larvae placed "right side up" might be sufficient to "evoke" actions reminiscent of a self-righting response. We developed an optogenetic system in which we activated SRN cells by means of *R54F03*-driven *Channelrhodopsin 2 (ChR2)* in trans-retinal fed larvae. Under blue light stimulation, larvae performed

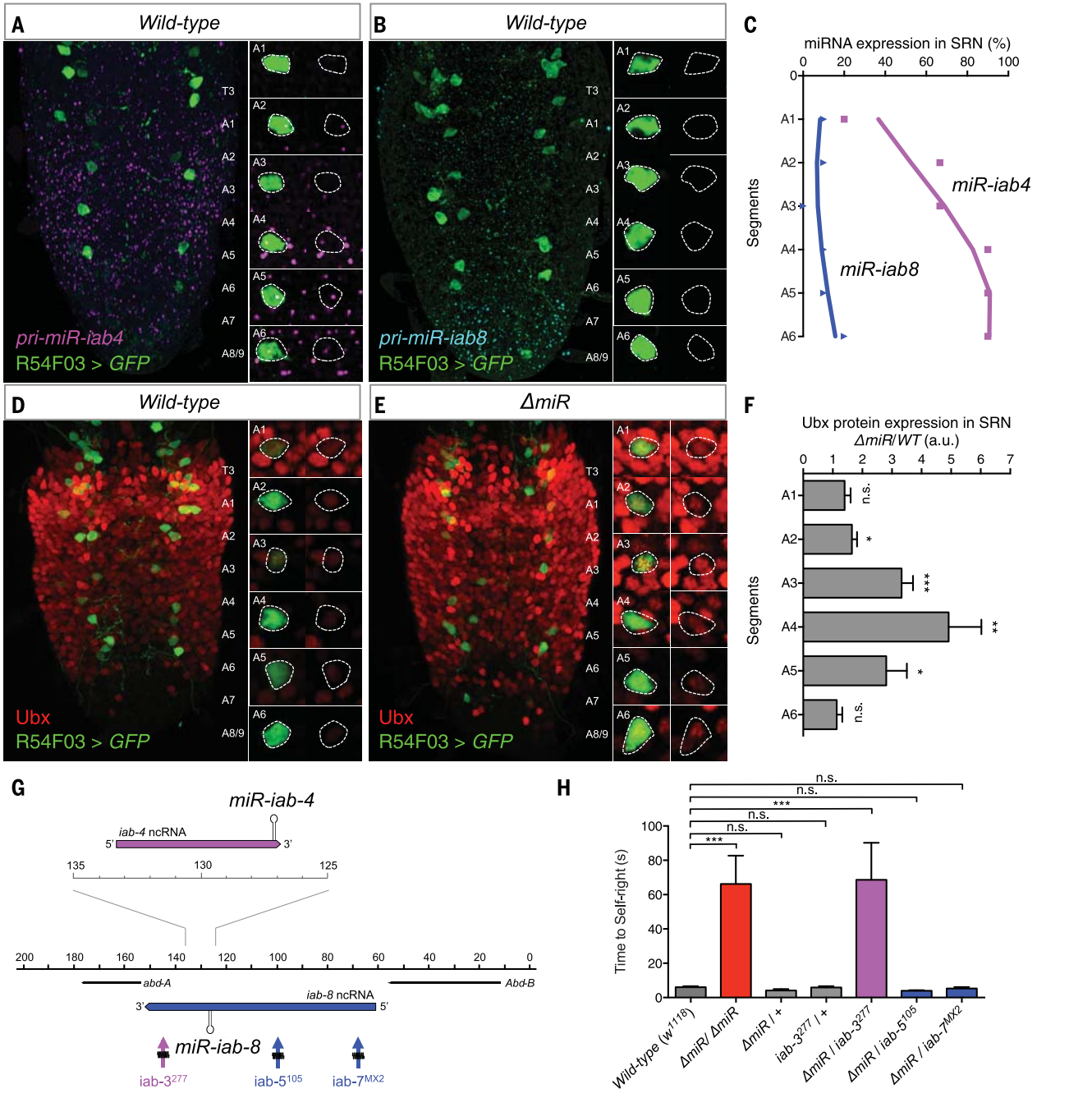

Fig. 3. Regulation of Ubx protein expression in SRN cells by *miR-iab4/iab8*. (**A**) Wild-type expression of precursor *miR-iab4* transcripts [RNA–fluorescence in situ hybridization (RNA-FISH), purple] in SRN cells (*R54F03*>GFP, green) of the ventral nerve cord (VNC) of first-instar *Drosophila* larvae. (**B**) Wild-type expression of precursor *miR-iab8* transcripts (RNA-FISH, blue) in SRN cells (R54F03>GFP, green) of the VNC of first-instar *Drosophila* larvae. (**C**) Percentage of SRN cells expressing *miR-iab4* (purple, square) and *miR-iab8* (blue, triangle) precursors across A1 to A6 ($n = 10$ larvae). (**D** and **E**) Ubx protein expression (red) in SRN cells of wild-type (D) and *ΔmiR* (E) first-instar larvae VNCs. (**F**) Quantification of Ubx protein expression ratio of *ΔmiR* over wild type within the SRN cells (red) by fluorescent intensity ($n = 8$ larvae per genotype; arbitrary units, a.u.). (**G**) Diagram of a subregion of the bithorax complex based on (*14*) showing *iab-4* (purple) and *iab-8* (blue) noncoding RNAs (ncRNAs), and rearrangement breakpoints affecting *miR-iab-4* (iab-3^{277}, purple) and *miR-iab-8* (iab-5^{105} and iab-7^{MX2}, blue). (**H**) Genetic complementation tests to determine the involvement of *miR-iab4* or *miR-iab8* in SR behavior by using trans-heterozygote larvae for *ΔmiR* and different chromosomal rearrangement breakpoints that disrupt the bithorax complex (mean ± SEM; $n = 17$ to 20 larvae per genotype). A nonparametric Mann-Whitney *U* test was performed to compare treatments; $P > 0.05$ (nonsignificant; n.s.); $^*P < 0.05$; $^{**}P < 0.01$; $^{***}P < 0.001$.

an atypical bending movement, frequently adopting a "lunette" position (fig. S7 and movie S5). Neither parental line *R54F03*-Gal4 nor UAS-*ChR2* showed similar reactions to stimulation, confirming the specificity of this effect (fig. S7 and movies S6 and S7).

To study the links between SRN neurons and the SR movement, we labeled SRN projections with *myr-GFP* and discovered that SRN cells

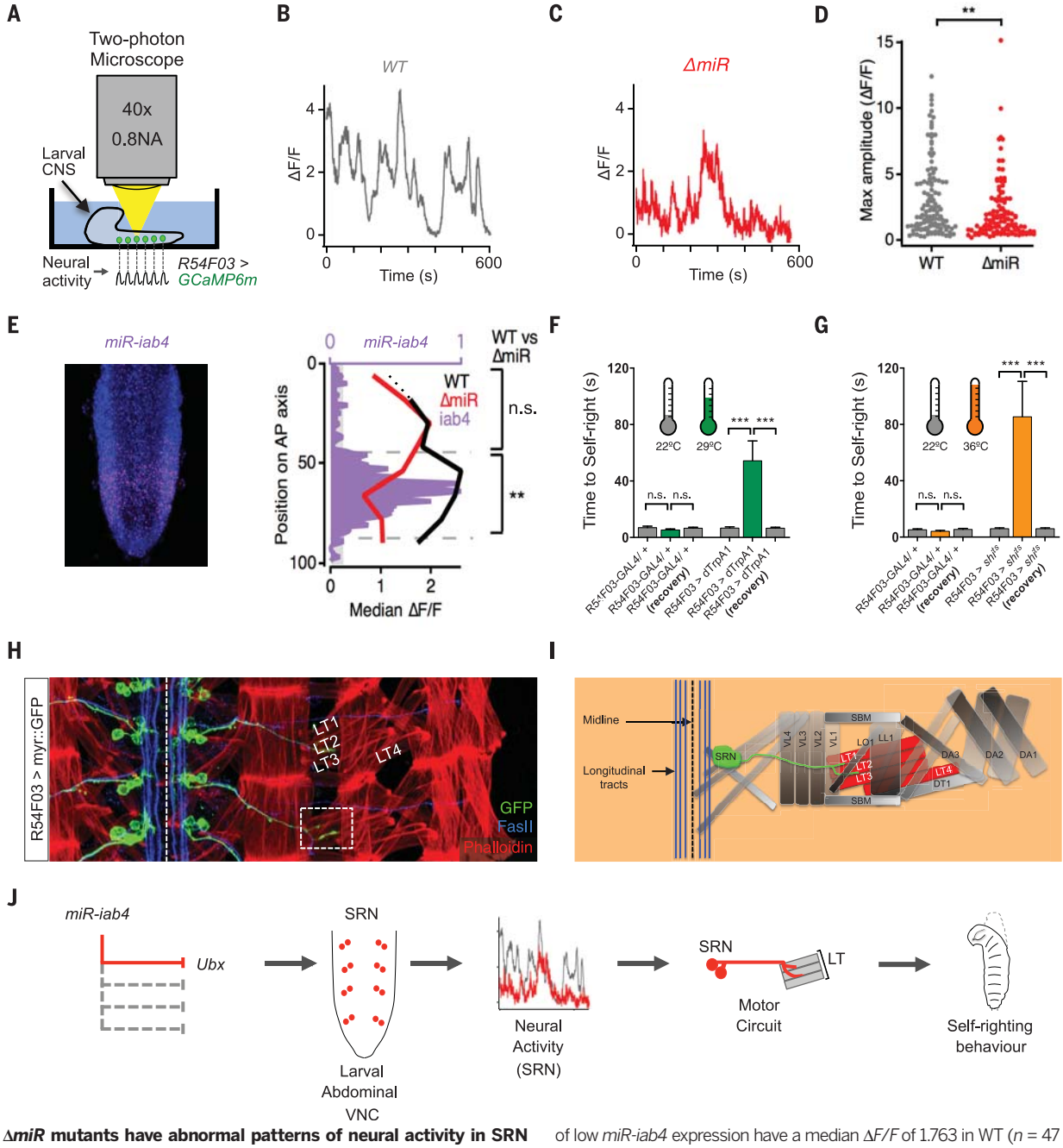

Fig. 4. Δ*miR* mutants have abnormal patterns of neural activity in SRN cells. (**A**) Schematic of the larval CNS expressing GCaMP6m in SRN cells (*R54F03> GCaMP6m*, green) imaged in a two-photon microscope. (**B**) Examples of spontaneous activity recorded over 10 min from wild type (WT: UAS-*GCaMP6m/+*; *R54F03*-GAL4/+) and (**C**) Δ*miR* mutants (UAS-*GCaMP6m/+*; *R54F03*-GAL4, Δ*miR*/Δ*miR*) in SRN cells. (**D**) Maximum amplitude of spontaneous activity in SRN cells: WT (median $\Delta F/F = 1.91$; $n = 120$ SRN cells) and in Δ*miR* mutants (median $\Delta F/F = 1.27$; $n = 115$ SRN cells) (**$P < 0.01$, Mann-Whitney *U* test). (**E**) Expression pattern of *miR-iab4* (purple) and 4′,6-diamidino-2-phenylindole (DAPI, blue) in the VNC of a freshly hatched larva (left). Median $\Delta F/F$ in SRN cells of WT (black line) and Δ*miR* (red line) larval VNCs, and relative expression of *miR-iab4* (purple) along the anterior-posterior (A-P) axis. Median $\Delta F/F$ of WT (median of 2.132, $n = 73$ SRN cells) and Δ*miR* (median of 1.122, $n = 68$ SRN cells) in regions of high *miR-iab4* expression (**$P < 0.01$, Mann-Whitney *U* test). Regions of low *miR-iab4* expression have a median $\Delta F/F$ of 1.763 in WT ($n = 47$ SRN cells) and 1.749 ($n = 47$ SRN cells) in Δ*miR* specimens (n.s., $P > 0.05$; Mann-Whitney *U* test). (**F** and **G**) Thermogenetic manipulation of neural activity in SRN cells. Activation [(F), *R54F03>dTrpA1*] and inhibition [(G), *R54F03>shi^{ts}*] of SRN neural activity (mean ± SEM; $n = 17$ larvae per genotype, ***$P < 0.0001$, Mann-Whitney *U* test) [29°C (green) for activation (H) and 36°C (orange) for inhibition (I)]. (**H**) Wild-type motor axonal projections of SRN cells (UAS-*myr::GFP*/UAS-*myr::GFP*; *R54F03*-GAL4/*R54F03*-GAL4, green) into muscles (phalloidin, red) lateral transverse 1 and 2 (LT1 and LT2) in late embryos (stage 17) (Fasciclin II, FASII, blue). Scale bars, 10 μm. (**I**) Diagram of SRN cells projecting to the LT1 and LT2 muscles. (**J**) A model that summarizes the data reported in this study. Mutation of *miR-iab4* (left) leads to Ubx derepression in the SRN node, affecting SRN neural activity patterns and triggering an anomalous SR behavior (right).

innervate two of the lateral transverse (LT) muscles and that they can be colabeled with antibodies against Fasciclin 2 (Fas2) (Fig. 4H), demonstrating these to be motorneurons. LT muscles are innervated by Bar-H1^{+} motorneurons (fig. S8A), so we used *Bar-H1*-Gal4 as a second driver to demonstrate that appropriate Ubx levels in these cells are required for normal SR behavior (fig. S8B), establishing the SRN cells as the LT-MNs.

We have therefore shown that miRNA-dependent *Hox* gene repression within a distinct group of motorneurons (SRN/LT-MNs) is required for the control of a specific locomotor behavior in the early *Drosophila* larva. Our finding that *Hox* gene posttranscriptional regulation is involved in SR control suggests that other RNA-based regulatory processes affecting *Hox* gene expression might also impinge on specific neural outputs; we are currently investigating this possibility, with special regard to the roles of the *Hox* genes in the specification of neural lineages with axial-specific architectures, and systematically testing the roles of other miRNAs on behavior.

That we could not detect any obvious neuroanatomical changes in miRNA mutant embryos suggests that these are either very subtle or that the role of miRNA regulation may be primarily behavioral, in the sense of affecting the performance of a correctly wired neural system, rather than developmental, contributing to the development of the network (*26*). Given that *miR-iab4/iab8* is involved in adult ovary innervation (*16*), it seems that miRNAs—much like ordinary protein-coding genes—can be involved in several distinct roles within the organism.

The results of this study contribute to the understanding of how complex innate behaviors are represented in the genetic program. Our data lead us to propose that other miRNAs might also be involved in the control of behavior in *Drosophila* and other species.

REFERENCES AND NOTES

1. D. P. Bartel, *Cell* **136**, 215–233 (2009).
2. X. Li, P. Jin, *Nat. Rev. Neurosci.* **11**, 329–338 (2010).
3. A. X. Sun, G. R. Crabtree, A. S. Yoo, *Curr. Opin. Cell Biol.* **25**, 215–221 (2013).
4. S. Thomsen, G. Azzam, R. Kaschula, L. S. Williams, C. R. Alonso, *Development* **137**, 2951–2960 (2010).
5. H. C. Reed *et al.*, *Genetics* **184**, 745–758 (2010).
6. L. F. de Navas *et al.*, *Development* **138**, 107–116 (2011).
7. A. Rogulja-Ortmann *et al.*, *Development* **141**, 2046–2056 (2014).
8. W. McGinnis, R. Krumlauf, *Cell* **68**, 283–302 (1992).
9. R. K. Maeda, F. Karch, *Development* **133**, 1413–1422 (2006).
10. M. Mallo, C. R. Alonso, *Development* **140**, 3951–3963 (2013).
11. M. Ronshaugen, F. Biemar, J. Piel, M. Levine, E. C. Lai, *Genes Dev.* **19**, 2947–2952 (2005).
12. D. M. Tyler *et al.*, *Genes Dev.* **22**, 26–36 (2008).
13. A. Stark *et al.*, *Genes Dev.* **22**, 8–13 (2008).
14. W. Bender, *Genes Dev.* **22**, 14–19 (2008).
15. M. Gummalla *et al.*, *PLOS Genet.* **8**, e1002720 (2012).
16. D. L. Garaulet *et al.*, *Dev. Cell* **29**, 635–648 (2014).
17. C. B. Bridges, T. H. Morgan, *The Third-Chromosome Group of Mutant Characters of* Drosophila melanogaster (Carnegie Institution of Washington, Baltimore, MD, 1923).
18. E. Sánchez-Herrero, I. Vernós, R. Marco, G. Morata, *Nature* **313**, 108–113 (1985).
19. B. D. Pfeiffer *et al.*, *Proc. Natl. Acad. Sci. U.S.A.* **105**, 9715–9720 (2008).
20. L. Manning *et al.*, *Cell Rep.* **2**, 1002–1013 (2012).
21. T.-W. Chen *et al.*, *Nature* **499**, 295–300 (2013).
22. M. Gummalla, S. Galetti, R. K. Maeda, F. Karch, *Front. Cell. Neurosci.* **8**, 96 (2014).
23. F. Karch *et al.*, *Cell* **43**, 81–96 (1985).
24. F. N. Hamada *et al.*, *Nature* **454**, 217–220 (2008).
25. T. Kitamoto, *J. Neurobiol.* **47**, 81–92 (2001).
26. S. Brenner, *Genetics* **77**, 71–94 (1974).

ACKNOWLEDGMENTS

We thank L. Lagnado for his support to this project and S. Pinho and P. Reed for technical assistance. We also thank R. White for antibodies; Welcome Bender, E. Sánchez-Herrero, and the Bloomington Stock Centre for *Drosophila* stocks; and P. Patraquim for bioinformatic support. This paper is dedicated to the memory of Amalia Lamuedra de Alonso for her devoted support to this work. This research was funded by a Wellcome Trust Investigator Award to C.R.A. [WT grant 098410/Z/12/Z] and a Ph.D. studentship to J.P.O. by Fundação para a Ciência e a Tecnologia (Portugal) [FCT grant SFRH/BD/63312/2009]. J.B. is funded by Sir Henry Dale Fellowship (Wellcome Trust and the Royal Society) Grant 105568/Z/14/Z, and M.L. was supported by grants from the Biotechnology and Biological Sciences Research Council (UK) (BB/I022414/1) and the Wellcome Trust (092986/Z).

SUPPLEMENTARY MATERIALS

www.sciencemag.org/content/350/6262/815/suppl/DC1
Materials and Methods
Figs. S1 to S11
References (*27*–*48*)
Movies S1 to S7

24 July 2015; accepted 25 September 2015
Published online 22 October 2015
10.1126/science.aad0217

HUMAN EVOLUTION

Ancient Ethiopian genome reveals extensive Eurasian admixture throughout the African continent

M. Gallego Llorente,[1*†] E. R. Jones,[2*†] A. Eriksson,[1,3] V. Siska,[1] K. W. Arthur,[4] J. W. Arthur,[4] M. C. Curtis,[5,6] J. T. Stock,[7] M. Coltorti,[8] P. Pieruccini,[8] S. Stretton,[9] F. Brock,[10,11] T. Higham,[10] Y. Park,[12] M. Hofreiter,[13,14] D. G. Bradley,[2] J. Bhak,[15] R. Pinhasi,[16*‡] A. Manica[1*‡]

Characterizing genetic diversity in Africa is a crucial step for most analyses reconstructing the evolutionary history of anatomically modern humans. However, historic migrations from Eurasia into Africa have affected many contemporary populations, confounding inferences. Here, we present a 12.5× coverage ancient genome of an Ethiopian male ("Mota") who lived approximately 4500 years ago. We use this genome to demonstrate that the Eurasian backflow into Africa came from a population closely related to Early Neolithic farmers, who had colonized Europe 4000 years earlier. The extent of this backflow was much greater than previously reported, reaching all the way to Central, West, and Southern Africa, affecting even populations such as Yoruba and Mbuti, previously thought to be relatively unadmixed, who harbor 6 to 7% Eurasian ancestry.

The ability to sequence ancient genomes has revolutionized our understanding of human evolution. However, genetic analyses of ancient material have focused on individuals from temperate and Arctic regions, where ancient DNA is preserved over longer time frames (*1*). Africa has so far failed to yield skeletal remains with much ancient DNA, with the exception of a few poorly preserved specimens from which only mitochondrial DNA could be extracted (*2*). This is particularly unfortunate, as African genetic diversity is crucial to most analyses reconstructing the evolutionary history of anatomically modern humans, by providing the baseline against which other events are defined. In the absence of ancient DNA, geneticists rely on contemporary African populations, but a number of historic events, in particular a genetic backflow from West Eurasia into Eastern Africa (*3*, *4*), act as confounding factors.

Here, we present an ancient human genome from Africa and use it to disentangle the effects of recent population movement into Africa. By sampling the petrous bone (*5*), we sequenced the genome of a male from Mota Cave (herein referred to as "Mota") in the southern Ethiopian highlands, with a mean coverage of 12.5× (*6*). Contamination was estimated to be between 0.29 and 1.26% (*6*). Mota's remains were dated to ~4500 years ago [direct calibrated radiocarbon date (*6*)] and thus predate both the Bantu expansion (*7*) and, more importantly, the 3000-year-old West Eurasian backflow, which has left strong genetic signatures in the whole of Eastern and, to a lesser extent, Southern Africa (*3*, *4*).

We compared Mota to contemporary human populations (*6*). Both principal component analysis (PCA) (Fig. 1A) and outgroup f_3 analysis using Ju|'hoansi (Khoisan) from Southern Africa as the outgroup (Fig. 1, B and C) place this ancient

MicroRNA-encoded behavior in *Drosophila*

Joao Picao-Osorio, Jamie Johnston, Matthias Landgraf, Jimena Berni and Claudio R. Alonso (October 22, 2015)

Science **350** (6262), 815-820. [doi: 10.1126/science.aad0217]
originally published online October 22, 2015

Editor's Summary

MicroRNAs that control behavior

MicroRNAs (miRNAs) are small non-coding RNAs that regulate gene activity. They repress expression through complementary base pairing interactions with target messenger RNAs. MiRNAs are involved in regulating many cell and developmental processes. Picao-Osorio *et al*. find that miRNAs can also control behavior in the fruit fly *Drosophila*. A specific miRNA locus regulates the self-righting response in larva that ate tipped over onto their backs. The miRNA locus targets a gene required for the normal activity of two neurons involved in the self-righting response.

Science, this issue p. 815

Science (print ISSN 0036-8075; online ISSN 1095-9203) is published weekly, except the last week in December, by the American Association for the Advancement of Science, 1200 New York Avenue NW, Washington, DC 20005.